



Supplementary Materials for
Engineered bacteria detect tumor DNA

Robert M. Cooper *et al.*

Corresponding authors: Susan L. Woods, susan.woods@adelaide.edu.au; Daniel L. Worthley, dan@colonoscopyclinic.com.au; Jeff Hasty, hasty@ucsd.edu

Science **381**, 682 (2023)
DOI: 10.1126/science.adf3974

The PDF file includes:

Materials and Methods
Figs. S1 to S8
References

Other Supplementary Material for this manuscript includes the following:

MDAR Reproducibility Checklist
Movie S1
Data File S1

Supplementary Materials

Materials and Methods

Bacterial cell culture and cloning to generate biosensors

Acinetobacter baylyi ADP1 was obtained from the American Type Culture Collection (ATCC #33305) and propagated in standard LB medium at 30 or 37 °C. *KRAS* homology arms were inserted into a neutral genetic locus denoted *Ntrl1*, replacing the gene remnant ACIAD2826. For the “large insert” design, a spectinomycin resistance gene was placed between the *KRAS* homology arms. For the “small insert” design, two stop codons were placed near the beginning of the *kanR* gene of the donor cassette, and the broken cassette was inserted into *A. baylyi*. CRISPR arrays were inserted into a neutral locus used previously (26), replacing ACIAD2186, 2187, and part of 2185. Ectopic CRISPR arrays were driven by a promoter region that included 684 bp from upstream of the first repeat of the endogenous, 90-spacer array.

For natural DNA biosensors, a temperature-sensitive *tetR* repressor was placed between the *KRAS* homology arms. An output gene, either *kanR* or GFP, was placed under control of the P_{LtetO-1} promoter in a second neutral locus denoted *Ntrl2*, replacing the gene remnants ACIAD1076-1077. Repeated attempts to clone wild type *tetR* into *A. baylyi* failed, but we fortuitously isolated a temperature sensitive mutant with two mutations: W75R and an additional 8 amino acids on the C terminus. This mutant *tetR* permitted growth at both 30 and 37 °C, but it only repressed its target at 30°C. The W75R mutant had been isolated previously in an intentional screen (38). We were able to clone wild-type *tetR* on the inducer aTc, but it was unable to grow without aTc at any temperature.

In vitro biosensor transformation experiments

A. baylyi were grown overnight in LB at 30 °C. Cells were then washed, resuspended in an equal volume of fresh LB, and mixed with donor DNA. For transformation in liquid, 50 µl cells were mixed with 250 ng donor DNA and incubated in a shaker at 30 °C for 2 hours or overnight. For transformation on agar, 2 µl cells were mixed with >50 ng donor DNA, spotted onto LB plates containing 2% wt/vol agar, and incubated at 30 °C overnight. Spots were cut out the next day and resuspended in 500 µl phosphate buffered saline solution (PBS). To count transformants, cells were 10-fold serially diluted 5 times, and 2 µl spots were deposited onto selective (30 ng/ml kanamycin) and non-selective 2% agar plates, with 3 measurement replicates at each dilution level. Larger volumes of undiluted samples were also spread onto agar plates to increase detection sensitivity (25 µl for liquid culture, 100 µl for resuspended agar spots). Colonies were counted at the lowest countable dilution level after overnight growth at 30 °C, and measurement replicates were averaged. Raw, unpurified lysate was produced by growing donor RKO cells in a culture dish until confluence, trypsinizing and harvesting cells, pelleting them in a 15 ml tube, resuspending them in 50 µl PBS, and placing the tube in a -20 °C freezer overnight to disrupt cell membranes.

In vitro statistics

Hypothesis testing was performed using two sample, one-sided t-tests in Matlab after taking base 10 logarithms, since serial dilutions produce log-scale data. Where data points were below

the limit of detection, they were replaced by the limit of detection as the most conservative way to include them in log-scale analysis. Comparisons between large vs small inserts or liquid vs solid agar culture were performed using paired t-tests, where data were matched for donor DNA and either culture type (liquid vs agar) or insert size, respectively. For Figure 2, D-G) n=4, I & J) n=5 except for random spacer n=3.

Creation of RKO, LS174T and SW620 donor cell lines

To create RKO donor and LS174T donor cell lines, lentiviral expression plasmid pD2119-FLuc2 KRasG12D donor was co-transfected with viral packaging vectors, psPAX2 (Addgene; plasmid; 12260) and MD2G (Addgene; plasmid; 12259), into HEK293T cells. At 48 and 72 h after transfection, viral supernatants were harvested, filtered through a 0.45- μ m filter, and concentrated using Amicon Ultra Centrifugal Filters (Merck Millipore; UFC910024). Concentrated lentivirus particles were used for transduction. The viral supernatant generated was used to transduce RKO, LS174T and SW620 cells. 48 hours after transduction, stable transformants were selected with 4 μ g/ml puromycin. Cell line identity was confirmed by STR analysis. KRAS status of RKO (*KRAS* wildtype), LS174T (*KRAS G12D*) and SW620 (*KRAS G12V*) cell lines was confirmed by amplification of a 220bp PCR fragment of the exon 2 *KRAS* gene, including codons 12 and 13 with primers *KRAS* F: GGTGGAGTATTTGATAGTGTATTAACC and *KRAS* R: AGAATGGTCCTGCACCAGTAA. Sanger sequencing was conducted using the same primers.

Creation of CRC donor organoids

BTRZI (*Braf*^{V600E}; *Tgfr2* ^{Δ/Δ} ; *Rnf43* ^{Δ/Δ} ; *Znf43* ^{Δ/Δ} ; *p16 Ink4a* ^{Δ/Δ}) organoids were generated using CRISPR-Cas9 engineering and grown in 50 μ l domes of GFR-Matrigel (Corning; 356231) in organoid medium: Advanced Dulbecco's modified Eagle medium/F12 (Gibco; 12634010) supplemented with 1x gentamicin/antimycotic/antibiotic (Gibco; 15710064, 15240062), 10mM HEPES (Gibco; 15630080), 2 mM GlutaMAX (Gibco; 35050061), 1x B27 (Gibco; 12504-044), 1x N2 (Gibco; 17502048), 50 ng/ml mouse recombinant EGF (Peprotech; 315-09), 10 ng/ml human recombinant TGF- β 1 (Peprotech; 100-21) (27). Following each split, organoids were cultured in 10 μ M Y-27632 (MedChemExpress; HY-10583), 3 μ M iPSC (Calbiochem; 420220), 3 μ M GSK-3 inhibitor (XVI, Calbiochem; 361559) for the first 3 days. Human colorectal tumor samples were obtained at the time of surgery for routine pathological analysis. All participants gave written informed consent and research was conducted in accordance with the Declaration of Helsinki, the NHMRC Statement on Ethical Conduct in Human Research, and institutional approval (HREC/16/SAC/344 SSA/18/CALHN/71). Tumor organoid lines were derived as previously described with minor modifications (39). Tissue samples were first minced and enzymatically digested in organoid digestion medium containing advanced DMEM-F12 (Gibco; 12634-010), Antibiotic-Antimycotic (Gibco; 15240-062), 50 μ g/ml Gentamicin (Gibco; 15750-060), 1% FCS, Collagenase IV 75 U/ml (Gibco; 17104019), Dispase 125 μ g/ml (Gibco; 17105-041), Hyaluronidase 20 μ g/ml (Sigma; H3506), Y27632 (Sigma; Y0503) in a water bath at 37 $^{\circ}$ C for 10 minutes then a further 30 minutes shaking at 150 rpm in an orbital shaker at 37 $^{\circ}$ C. Samples were strained, washed and plated in domes of GFR-Matrigel (Corning; 356231). Human CRC organoids were cultured in colorectal

cancer medium containing advanced DMEM/F12 (Gibco; 12634-010), Antibiotic-Antimycotic (Gibco; 15240-062), 50 µg/ml Gentamicin (Gibco; 15750-060), 10 mM HEPES (Sigma; H0887), 1x glutamax (Gibco; 35050-061), 2x B27 (Gibco; 17504044), 500 nM A83-01 (Tocris; 2939), 50 ng/ml hEGF (Sigma; SRP3027), 1 nM [Leu15]-Gastrin 1 (Sigma; G9145), 1 mM N-Acetyl-Lcysteine (Sigma; A9165), 5 µM SB202190 (Sigma; S7067), 10 µM SB431542 (Sigma; S4317), and 10 µM Y27632 (Sigma; Y0503). Colorectal cancer medium was changed twice weekly, with growth monitored until passaging was required.

To create CRC donor organoids, lentiviral expression plasmid pD2119-FLuc2 *KRASG12D* donor was co-transfected with viral packaging vectors, psPAX2 (Addgene; plasmid; 12260) and MD2G (Addgene; plasmid; 12259), into HEK293T cells. At 48 and 72 h after transfection, viral supernatants were harvested, filtered through a 0.45-µm filter, and concentrated using Amicon Ultra Centrifugal Filters (Merck Millipore; UFC910024). Concentrated lentivirus particles were used for transduction. The viral supernatant generated was used to transduce human CRC and BTRZI organoids by spinoculation. Briefly, organoids were dissociated to single cells using TrypLE. 1×10^5 single cells were mixed with 250 µl organoid medium; 10 µM Y-27632; 250 µl concentrated viral supernatant and 4 µg/ml polybrene (Sigma; H9268) in a 48 well tray before centrifugation at 600g for 90 minutes at 32 °C. Meanwhile, 120 µl 50:50 ADMEM:Matrigel mixture was added to a cold 24-well tray before centrifugation of this bottom Matrigel layer for 40 minutes at 200g at room temperature, followed by solidifying the Matrigel by incubating at 37 °C for 30 minutes. After spinoculation, cells were scraped from the well and plated on top of the Matrigel monolayer with organoid medium. The following day, the medium was removed and the upper layer of Matrigel was set over the organoids by adding 120 µl 50:50 ADMEM:Matrigel and allowing to set for 30 minutes before adding organoid medium. 48 hours after transduction, BTRZI donor organoids were selected with 8 µg/ml puromycin (Sigma; P8833) for 1 week, then maintained in organoid medium with 4 µg/ml puromycin. Human CRC donor organoids were selected and maintained in 4 µg/ml puromycin.

Calculating number of copies of target DNA integrated into cell lines and organoids

Genomic DNA (gDNA) was extracted from 5×10^6 cells using Purelink genomic DNA minikit (Invitrogen; K18200). Primer/probe sets were designed to amplify the human *KRAS* homology arms within the donor construct. 5'*KRAS* homologyArm FWD 5'- CAG AAC AGC AGT CTG GCT ATT TA-3'; 5'*KRAS* homologyArm REV 5'- ACT GCA GAC GTG TAT CGT AAT G - 3' and 5' *KRAS* homologyArm PRB 5'-/56-FAM/AGC GTC GAT /ZEN/GGA GGA GTT TGT AAA TGA/31ABkFQ/-3'. Quantitative PCR (qPCR) reactions were optimized with normal human gDNA (from PBMC), mouse gDNA (BTRZI parental organoid gDNA) and BTRZI donor gDNA to show that primer/probe sets amplify both endogenous human *KRAS* and the donor construct, but not mouse *Kras*. To enable calculation of copy number of each cell and organoid line, a standard curve was generated with normal human gDNA (2-fold serial dilution 100 ng to 3.125 ng per qPCR reaction). qPCR was conducted on 25 ng gDNA from organoids and cell lines. All qPCR reactions were normalized to 100 ng per qPCR reaction with mouse gDNA (BTRZI parental organoid gDNA) and used KAPA probe fast universal (Roche; KK4703).

Organoid lysate mixed with *A. baylyi* sensor bacteria

BTRZI (parental) and BTRZI donor organoids were grown for 5 days in 50 μ l GFR-Matrigel domes. Organoids were dissociated to single cells with TrypLE, counted and 6×10^5 single cells were collected in PBS and snap frozen. The CFU equivalence of exponentially growing *A. baylyi* sensor culture at OD₆₀₀ 0.35 was ascertained by serial dilution of 3 independent cultures with 5 technical replicates plated on 10 μ g/ml chloramphenicol LB agar plate to be 2.4×10^8 CFU per ml. *A. baylyi* sensor was grown in liquid culture with 10 μ g/ml chloramphenicol to OD₆₀₀ 0.35 before mixing with organoid lysate at a 1:1 ratio and grow overnight on LB agar plates at 30 °C. All bacteria were scraped into 200 μ l LB/20% glycerol before spotting 5x 5 μ l spots onto kanamycin (Sigma; K1377) and chloramphenicol (Sigma; C0378) plates and grown overnight at 37 °C. Colonies were counted and the dilution factor was accounted for to calculate CFU per ml. Rate of HGT was calculated by dividing the CFU per ml of transformants (kanamycin plates) by the CFU per ml of total *A. baylyi* (chloramphenicol plates) for 5 independent experiments.

Coculture organoids with *A. baylyi* sensor bacteria

For co-culture experiments, 24-well trays were coated with Matrigel monolayers. Briefly, 200 μ l 50:50 ADMEM:Matrigel mixture was added to a cold 24-well tray and centrifuged for 40 minutes at 200xg at room temperature, followed by a 30-minute incubation at 37 °C to solidify Matrigel. BTRZI (parental) and BTRZI donor organoids were dissociated into small clusters using TrypLE and grown for 5 days on a Matrigel monolayer in organoid medium without antibiotics before 50 μ l OD₆₀₀ 0.35 *A. baylyi* sensor was added to each well. After 24 hours, organoids were photographed then collected and grown overnight on LB agar plates at 30 °C. All bacteria were scraped into 200 μ l LB/20% glycerol before spotting 5x 5 μ l spots onto kanamycin and chloramphenicol plates and grown overnight at 37 °C. Colonies were counted and the dilution factor was accounted for to calculate CFU per ml. Rate of HGT was calculated by dividing the CFU per ml of transformants (kanamycin plates) by the CFU per ml of total *A. baylyi* (chloramphenicol plates) for 5 independent experiments.

Horizontal gene transfer in vivo

BTRZI donor organoids were isolated from Matrigel and dissociated into small clusters using TrypLE. The cell clusters (equivalent to ~150 organoids per injection) were washed three times with cold PBS containing 10 μ M Y-27632 and then resuspended in 20 μ l 10% GFR Matrigel 1:1000 Indian ink, 10 μ M Y-27632 in PBS and orthotopically injected into the mucosa of the proximal and distal colon of anaesthetized 10- to 13-week-old NSG mice (150 organoids per injection), as previously described (27). Briefly, a customized needle (Hamilton Inc. part number 7803-05, removable needle, 33 gauge, 12 inches long, point 4, 12° bevel) was used. In each mouse up to 2 injections of 20 μ l were performed. CRC donor tumor growth was monitored by colonoscopy for 5 weeks and the videos were viewed offline using QuickTime Player for analysis. Colonoscopy was performed using a Karl Storz Image 1 Camera System comprised of: Image1 HDTV HUB CCU; Cold Light Fountain LED Nova 150 light source; Full HD Image1 3 Chip H3-Z Camera Head; Hopkins Telescope, 1.9mm, 0 degrees. A sealed Luer Lock was placed on the working channel of the telescope sheath to ensure minimal air leakage (Coherent Scientific; 14034-40). Tumor growth of the largest tumor visualized was

scored as previously described using the Becker Scale (40). All study groups were housed in separate cages. *A. baylyi* sensor was grown in LB liquid culture with 6 µg/ml chloramphenicol to OD₆₀₀ 0.6. *A. baylyi* parental was grown in LB liquid culture to OD₆₀₀ 0.6. *A. baylyi* was washed twice with PBS before 13 mice received 4x10¹⁰ *A. baylyi* sensor via enema (5 mice without tumors; 3 mice with non-donor BTRZI CRC tumors and 5 mice with BTRZI CRC donor tumors), 4 mice received 4x10¹⁰ *A. baylyi* parental via enema. Enema was performed as per previous publication (41). Briefly, mice were anesthetized with isoflurane and colon flushed with 1 ml of room temperature sterile PBS to clear the colon cavity of any remaining stool. A P200 pipette tip coated with warm water was then inserted parallel into the lumen to deliver 50 µl of bacteria into the colon over the course of 30 seconds. After infusion, the anal verge was sealed with Vetbond Tissue Adhesive (3M; 1469SB) to prevent luminal contents from being immediately excreted. Animals were maintained on anesthesia for 5 minutes, and then allowed to recover on heat mat and anal canal inspected 6 hours after the procedure to make sure that the adhesive has been degraded. 24 hours after *A. baylyi* administration, mice received a second enema dosing. Mice were then euthanized; colons were removed and luminal contents were collected. Luminal contents were grown overnight at 37 °C on LB agar with 10 µg/ml vancomycin plates. All bacteria were collected into 250 µl LB/20% glycerol, vortexed and stored at -80 °C. 5x 5µl serial dilutions were spotted onto LB agar plates containing: 1, vancomycin (to detect total *A. baylyi* parental); 2, chloramphenicol; vancomycin (to detect total *A. baylyi* sensor) and 3, kanamycin; chloramphenicol; vancomycin (to detect recombined *A. baylyi* sensor). Colonies were counted and dilutions were factored to calculate CFU *A. baylyi* per mouse. For experiments analyzing *A. baylyi* in stool, BTRZI CRC donor tumors were established and monitored as described above. After 5 weeks of tumor growth, 9 mice received *A. baylyi* sensor enemas (5 mice without tumors; 4 mice with BTRZI CRC donor tumors) and 6 mice received *A. baylyi* parental enemas (3 mice without tumors and 3 mice with BTRZI CRC donor tumors). Stool was collected 24 hours after *A. baylyi* administration into 250 µl PBS/20% glycerol, vortexed and stored at -80 °C. Stool was analyzed on LB agar plates containing: 1, vancomycin (Sigma; PHR1732) (to detect total *A. baylyi* parental); 2, chloramphenicol; vancomycin (to detect total *A. baylyi* sensor) and 3, kanamycin; chloramphenicol; vancomycin (to detect recombined *A. baylyi* sensor). Colonies were counted and dilutions were factored to calculate CFU *A. baylyi* per mouse.

Sequencing gDNA from bacterial colonies grown on kanamycin plates

A. baylyi transformants were individually picked from kanamycin; vancomycin plates and grown in liquid culture LB supplemented with 25 µg/ml kanamycin, 10 µg/ml vancomycin and 6 µg/ml chloramphenicol. gDNA was extracted using purelink genomic DNA minikit (Invitrogen; K182001). Genomic regions of interest were amplified using Primestar Max DNA polymerase (Takara; R045A) and primers HGTpcrF: CAAAATCGGCTCCGTCGATACTA; HGTpcrR: TAGCATCACCTTCACCCTC and 16S 27Fa: AGAGTTTGATCATGGCTCAG; 16s 27Fc: AGAGTTTGATCCTGGCTCAG; 16S 1492R: CGGTTACCTTGTTACGACTT (16S 27Fa:16S 27Fc: 16S 1492R = 0.5:0.5:1). Sanger sequencing was conducted using the same primers.

Calculating the detection limit of CATCH in the presence of stool

Stools were collected from C57BL/6 mice bearing CRC tumors. A stool slurry was created by vortexing 10 mouse stools (average weight 0.017 g) in 830 μ l LB/20% glycerol for each experiment, then 100 μ l stool slurry could be added to each reaction containing the equivalent of 1 stool. Donor plasmid DNA was serially diluted (10-fold from 3 ng/ μ l to 30 fg/ μ l). *A. baylyi* sensor was grown in LB liquid culture with 6 μ g/ml chloramphenicol to OD₆₀₀ 0.6. 5×10^7 *A. baylyi* sensor was mixed with 100 μ l stool slurry or 100 μ l LB/20% glycerol with or without serially diluted donor plasmid DNA. Reactions were incubated at 37°C for 4 hours before serially diluting (10-fold) and spotting 5x 5 μ l spots onto 25 μ g/ml kanamycin; 10 μ g/ml vancomycin LB agar plates and 6 μ g/ml chloramphenicol; 10 μ g/ml vancomycin LB agar plates and grown overnight at 37 °C. Colonies were counted and the dilution factor was accounted for to calculate CFU per ml. Rate of HGT was calculated by dividing the CFU per ml of transformants (kanamycin plates) by the CFU per ml of total *A. baylyi* (chloramphenicol plates) for 5 independent experiments.

Supplementary figures

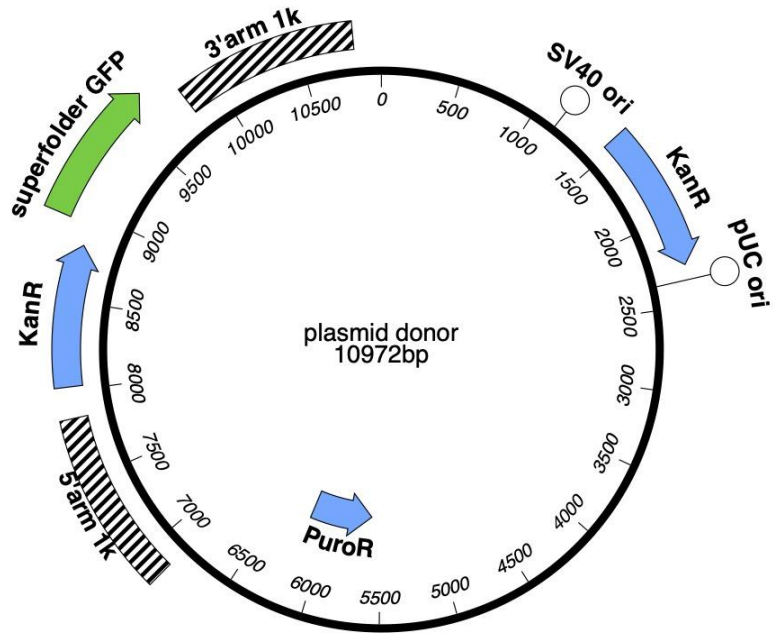


Figure S1: Engineered donor construct. Plasmid donor DNA used to transfect mammalian cell lines and as positive control donor DNA for in vitro experiments.

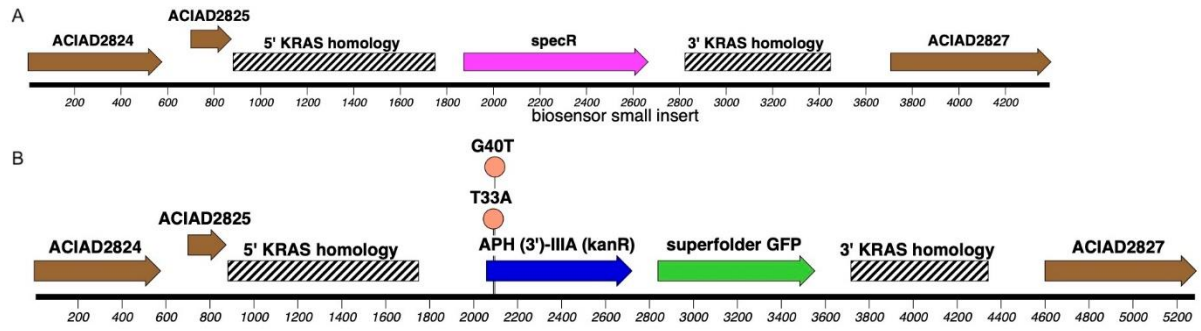


Figure S2: Engineered landing pad within the biosensor to receive target DNA. “Large insert” **A**, and “small insert” **B**, designs for the biosensors. *KRAS* homology arms are shown in striped, gray with surrounding genomic context outside them. Note that large and small inserts refer to the size of the donor DNA region that must transfer to confer kanamycin resistance, not to the size of the region between homology arms in the biosensor. Two single-base changes introducing nearby stop codons at the beginning of *kanR* are shown for the small insert design, **B**.

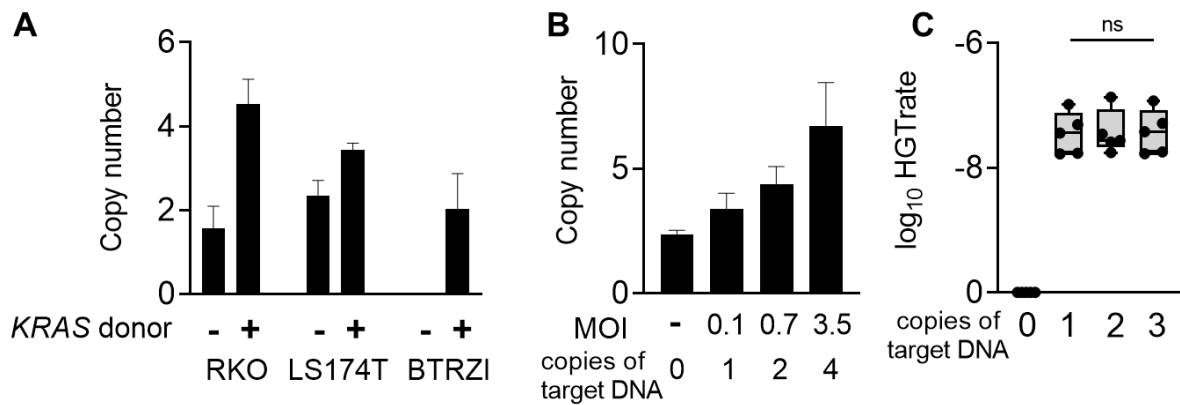


Figure S3: Copy number of target DNA within cancer cell and organoid lines. **A**, on average 1 to 3 copies of target donor DNA were integrated per cell into polyclonal donor cell and organoid lines. The number of copies of target donor DNA integrated per cell was quantitated using qPCR with primers designed to amplify the KRAS homology arms in the donor cassette, as well as endogenous human KRAS. Parental RKO and LS174T cell lines were diploid for human KRAS (2n), whereas human KRAS could not be amplified from parental BTRZI mouse organoid genomic DNA. Donor cells had endogenous KRAS locus (2n) as well as 2.5 ± 0.6 (RKO) and 1.4 ± 0.2 (LS174T) copies of target donor DNA. BTRZI donor organoids had 2.0 ± 0.8 copies of target donor DNA (mouse endogenous KRAS locus not detectable by human specific primers). $n=3$ independent gDNA extractions per sample with each qPCR conducted in triplicate and compared to a standard curve generated with normal human gDNA. **B**, LS174T cells were transduced with different multiplicity of infection (MOI) and stable cell lines were selected with $2 \mu\text{g/ml}$ puromycin. Donor cells had endogenous KRAS locus (2n) and 1.4 (MOI0.1), 2.4 (MOI0.7) and 4.7 (MOI3.5) copies of target donor DNA. **C**, Recombination with donor DNA from crude lysates of LS174T donor cell lines, with different numbers of target donor DNA integrated per cell, enables growth of *A. baylyi* sensor on kanamycin plates. $n=5$ independent experiments each with 5 technical replicates. Paired t-test showed that there was no significant difference in recombination efficiency.

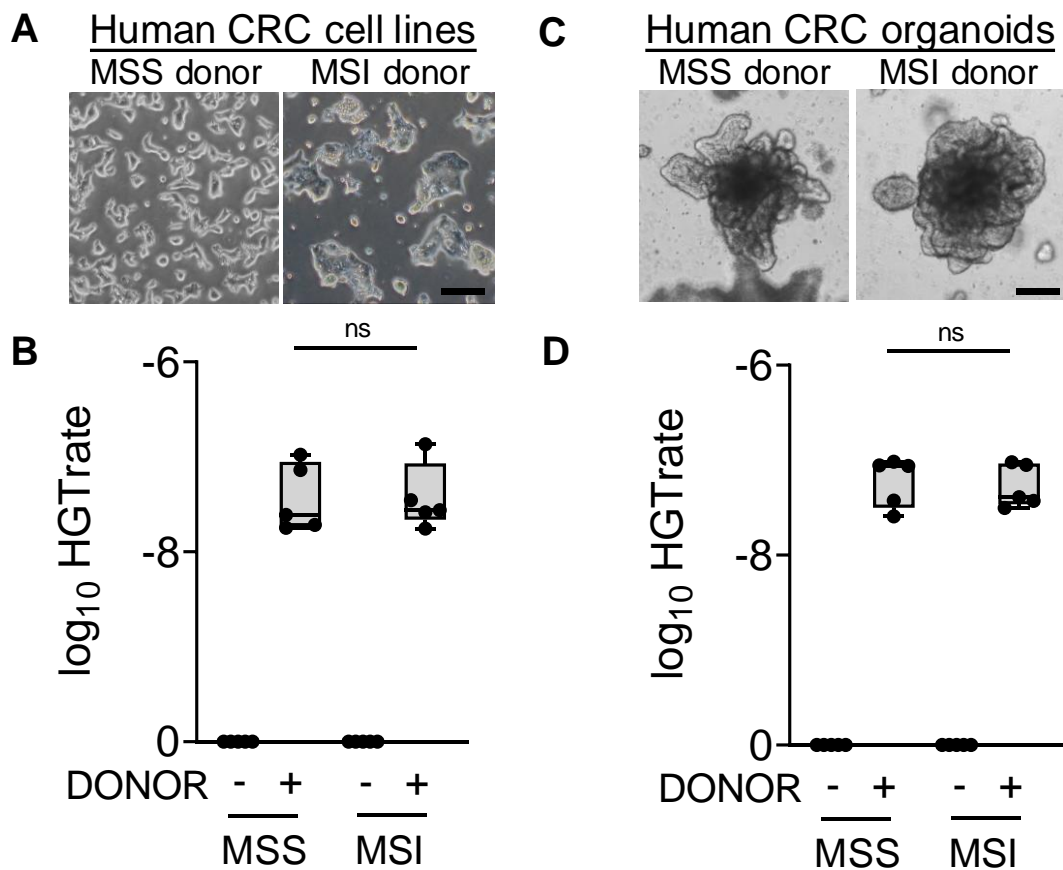


Figure S4: Detection of donor DNA from both MSS and MSI colorectal cell lines and human organoids. **A**, Images of human CRC cell lines, SW620 (MSS) and LS174T (MSI-H), with the donor cassette stably integrated into their genome. Scale bar 200 μm . **B**, Recombination with DNA from crude lysates of human CRC donor cell lines enables growth of *A. baylyi* sensor on kanamycin plates. **C**, Images of human CRC organoids established from patient surgical samples with the donor cassette stably integrated into their genome. Scale bar 200 μm . **D**, Recombination with DNA from crude lysates of human CRC donor organoid lines enables growth of *A. baylyi* sensor on kanamycin plates. In b and d, n=5 independent experiments each with 5 technical replicates. Paired t-test showed that there was no significant difference in recombination efficiency between MSS and MSI patient organoids.

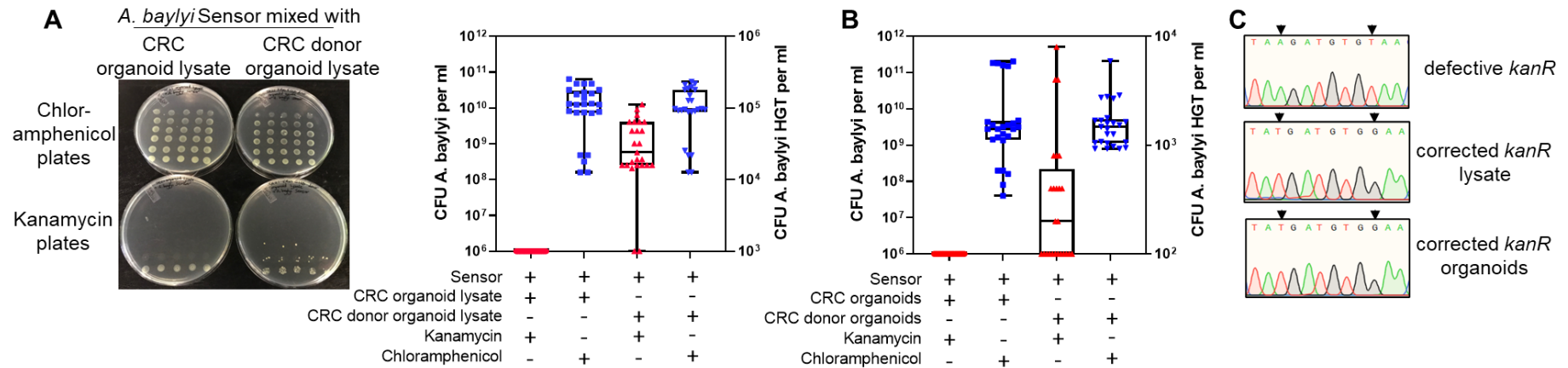


Figure S5: Sensor detection of donor DNA from BTRZI CRC organoids. *A. baylyi* sensor bacteria are constitutively chloramphenicol-resistant, hence *chlorR* CFUs provide a readout of total *A. baylyi* present. In contrast, kanamycin-resistant sensor bacteria rely on incorporation of donor DNA from CRC organoids to correct the defective *kanR* gene and enable growth on kanamycin selection plates. **A**, Recombination with lysate from CRC donor organoids enables growth of *A. baylyi* sensor on kanamycin plates. Shown here with representative plates and CFU analysis. **B**, after co-culturing established CRC donor organoids with *A. baylyi* sensor, recombination with donor DNA from CRC donor organoids enables growth of *A. baylyi* sensor on kanamycin plates. Shown here with representative images and CFU analysis. Scale bars 200 μ m. **A & B**, Fig 3 contains the same data as shown here but presented as HGT rate (kanamycin resistant CFU *A. baylyi* per ml/chloramphenicol CFU *A. baylyi* per ml), $n = 5$ independent experiments each with 5 technical replicates. **C** Representative Sanger sequencing chromatograms of PCR amplicon covering the region of the *kanR* gene containing informative SNPs, to highlight the difference in sequence in gDNA isolated from parental *A. baylyi* sensor bacteria compared to *A. baylyi* colonies isolated from kanamycin plates following mixing with donor organoid lysates or viable organoids.

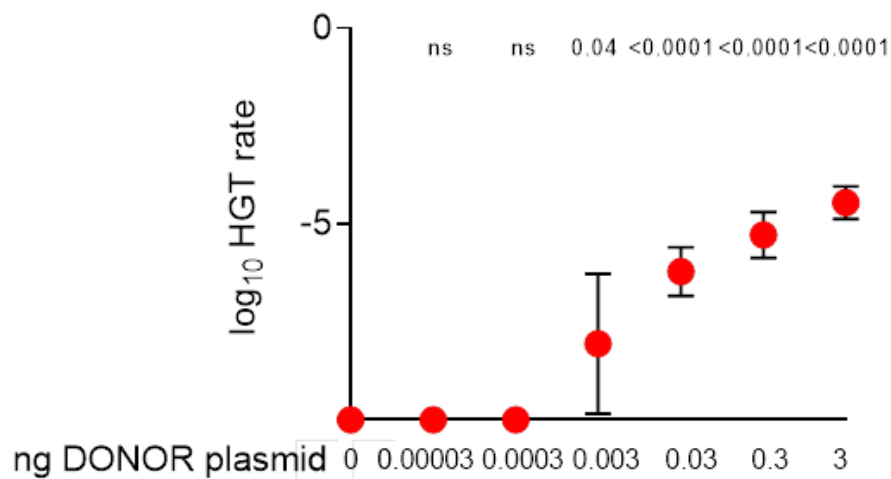


Figure S6: Detection of target DNA mixed with stool. *A. baylyi* sensor bacteria were mixed with serially diluted donor plasmid DNA in the presence of mouse stool collected from mice bearing CRC tumors (1 stool per reaction). After 3 hours of growth at 37 °C, serial dilutions of each reaction were plated onto kanamycin/vancomycin LB agar selection plates (*A. baylyi* sensor HGT) or chloramphenicol/vancomycin LB agar selection plates (total *A. baylyi* sensor). Rate of HGT was calculated (p-values calculated on log-transformed data using unpaired t-test). n=5 independent experiments, each with 5 technical replicates.

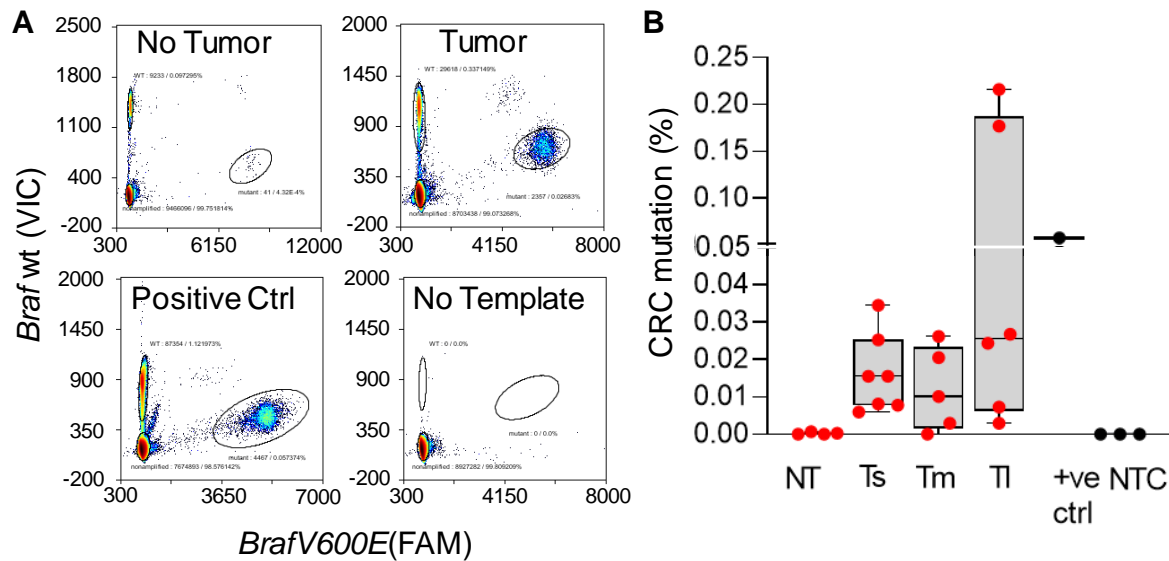


Figure S7: High sensitivity digital droplet PCR (ddPCR) detection of CRC mutation (*BrafV600E*) in stool DNA isolated from tumor-bearing animals. A, Representative images of ddPCR data. B, CRC mutation (*BrafV600E*) positive droplets as a % of total droplets. Analysis of no template negative control samples and stool DNA samples from non-tumor bearing animals was used to determine the sensitivity threshold of the assay. +ve ctrl = positive control samples that contains 10% *BrafV600E* gDNA spiked into stool DNA sample from a non-tumor bearing animal, NT = no tumor, Ts = small tumor, Tm = medium tumor, Tl = large tumor, NTC = no template PCR negative control (n=3-4 mice/group).

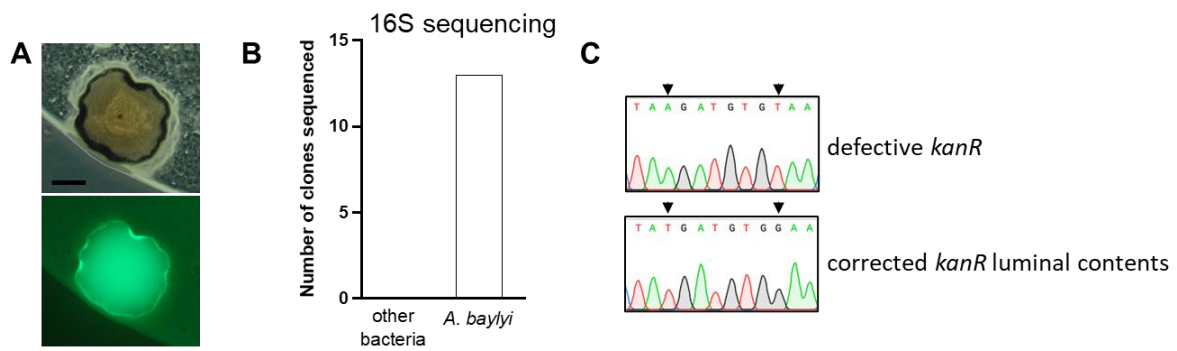


Figure S8: Horizontal gene transfer is detected in luminal contents from mice bearing BTRZI CRC donor tumors after rectal dosing of *A. baylyi* sensor bacteria. Recombined transformants were **A**, GFP positive and confirmed as *A. baylyi* by **B**, 16s sequencing on kanamycin/chloramphenicol/vancomycin selection plates, scale bar 500 μm . **C**, Representative Sanger sequencing chromatograms of PCR amplicon covering the region of the *kanR* gene containing informative SNPs to highlight the difference in sequencing DNA isolated from parental *A. baylyi* sensor bacteria compared to *A. baylyi* colonies isolated from kanamycin/chloramphenicol/vancomycin plates in luminal contents from mice bearing BTRZI CRC donor tumors after rectal dosing of *A. baylyi* sensor bacteria.

Movie S1: *A. baylyi* biosensors taking up plasmid donor DNA.

A. baylyi were grown overnight, washed into fresh LB, mixed with saturating pLenti-KRAS donor DNA, and sandwiched between an agar pad and a glass bottom dish. Images were taken every 10 minutes. GFP fluorescence indicates that the cells have taken up and genomically integrated the donor DNA cassette.

Supplementary Materials References

References and notes

1. S. Slomovic, K. Pardee, J. J. Collins, Synthetic biology devices for in vitro and in vivo diagnostics. *Proc. Natl. Acad. Sci. U.S.A.* **112**, 14429–14435 (2015). [doi:10.1073/pnas.1508521112](https://doi.org/10.1073/pnas.1508521112) [Medline](#)
2. F. Sedlmayer, D. Aubel, M. Fussenegger, Synthetic gene circuits for the detection, elimination and prevention of disease. *Nat. Biomed. Eng.* **2**, 399–415 (2018). [doi:10.1038/s41551-018-0215-0](https://doi.org/10.1038/s41551-018-0215-0) [Medline](#)
3. W. A. Lim, C. H. June, The Principles of Engineering Immune Cells to Treat Cancer. *Cell* **168**, 724–740 (2017). [doi:10.1016/j.cell.2017.01.016](https://doi.org/10.1016/j.cell.2017.01.016) [Medline](#)
4. D. T. Riglar, T. W. Giessen, M. Baym, S. J. Kerns, M. J. Niederhuber, R. T. Bronson, J. W. Kotula, G. K. Gerber, J. C. Way, P. A. Silver, Engineered bacteria can function in the mammalian gut long-term as live diagnostics of inflammation. *Nat. Biotechnol.* **35**, 653–658 (2017). [doi:10.1038/nbt.3879](https://doi.org/10.1038/nbt.3879) [Medline](#)
5. M. Mimee, P. Nadeau, A. Hayward, S. Carim, S. Flanagan, L. Jerger, J. Collins, S. McDonnell, R. Swartwout, R. J. Citorik, V. Bulović, R. Langer, G. Traverso, A. P. Chandrakasan, T. K. Lu, An ingestible bacterial-electronic system to monitor gastrointestinal health. *Science* **360**, 915–918 (2018). [doi:10.1126/science.aas9315](https://doi.org/10.1126/science.aas9315) [Medline](#)
6. N. Mao, A. Cubillos-Ruiz, D. E. Cameron, J. J. Collins, Probiotic strains detect and suppress cholera in mice. *Sci. Transl. Med.* **10**, eaao2586 (2018). [doi:10.1126/scitranslmed.aao2586](https://doi.org/10.1126/scitranslmed.aao2586) [Medline](#)
7. T. Danino, A. Prindle, G. A. Kwong, M. Skalak, H. Li, K. Allen, J. Hasty, S. N. Bhatia, Programmable probiotics for detection of cancer in urine. *Sci. Transl. Med.* **7**, 289ra84 (2015). [doi:10.1126/scitranslmed.aaa3519](https://doi.org/10.1126/scitranslmed.aaa3519) [Medline](#)
8. J. W. Kotula, S. J. Kerns, L. A. Shaket, L. Siraj, J. J. Collins, J. C. Way, P. A. Silver, Programmable bacteria detect and record an environmental signal in the mammalian gut. *Proc. Natl. Acad. Sci. U.S.A.* **111**, 4838–4843 (2014). [doi:10.1073/pnas.1321321111](https://doi.org/10.1073/pnas.1321321111) [Medline](#)
9. T. S. Gardner, C. R. Cantor, J. J. Collins, Construction of a genetic toggle switch in *Escherichia coli*. *Nature* **403**, 339–342 (2000). [doi:10.1038/35002131](https://doi.org/10.1038/35002131) [Medline](#)
10. A. Courbet, D. Endy, E. Renard, F. Molina, J. Bonnet, Detection of pathological biomarkers in human clinical samples via amplifying genetic switches and logic gates. *Sci. Transl. Med.* **7**, 289ra83 (2015). [doi:10.1126/scitranslmed.aaa3601](https://doi.org/10.1126/scitranslmed.aaa3601) [Medline](#)

11. J. C. Mell, R. J. Redfield, Natural competence and the evolution of DNA uptake specificity. *J. Bacteriol.* **196**, 1471–1483 (2014). [doi:10.1128/JB.01293-13](https://doi.org/10.1128/JB.01293-13) [Medline](#)
12. S. M. Soucy, J. Huang, J. P. Gogarten, Horizontal gene transfer: Building the web of life. *Nat. Rev. Genet.* **16**, 472–482 (2015). [doi:10.1038/nrg3962](https://doi.org/10.1038/nrg3962) [Medline](#)
13. K. M. Robinson, K. B. Sieber, J. C. Dunning Hotopp, A review of bacteria-animal lateral gene transfer may inform our understanding of diseases like cancer. *PLOS Genet.* **9**, e1003877 (2013). [doi:10.1371/journal.pgen.1003877](https://doi.org/10.1371/journal.pgen.1003877) [Medline](#)
14. J. C. Dunning Hotopp, Horizontal gene transfer between bacteria and animals. *Trends Genet.* **27**, 157–163 (2011). [doi:10.1016/j.tig.2011.01.005](https://doi.org/10.1016/j.tig.2011.01.005) [Medline](#)
15. D. M. Young, D. Parke, L. N. Ornston, Opportunities for genetic investigation afforded by *Acinetobacter baylyi*, a nutritionally versatile bacterial species that is highly competent for natural transformation. *Annu. Rev. Microbiol.* **59**, 519–551 (2005). [doi:10.1146/annurev.micro.59.051905.105823](https://doi.org/10.1146/annurev.micro.59.051905.105823) [Medline](#)
16. R. Palmen, B. Vosman, P. Buijsman, C. K. D. Breek, K. J. Hellingwerf, Physiological characterization of natural transformation in *Acinetobacter calcoaceticus*. *J. Gen. Microbiol.* **139**, 295–305 (1993). [Medline](#)
17. T.-L. Chen, L.-K. Siu, Y.-T. Lee, C.-P. Chen, L.-Y. Huang, R. C.-C. Wu, W.-L. Cho, C.-P. Fung, *Acinetobacter baylyi* as a pathogen for opportunistic infection. *J. Clin. Microbiol.* **46**, 2938–2944 (2008). [doi:10.1128/JCM.00232-08](https://doi.org/10.1128/JCM.00232-08) [Medline](#)
18. L. Nordgård, T. Nguyen, T. Midtvedt, Y. Benno, T. Traavik, K. M. Nielsen, Lack of detectable DNA uptake by bacterial gut isolates grown in vitro and by *Acinetobacter baylyi* colonizing rodents in vivo. *Environ. Biosafety Res.* **6**, 149–160 (2007). [doi:10.1051/ebr:2007029](https://doi.org/10.1051/ebr:2007029) [Medline](#)
19. R. M. Cooper, L. Tsimring, J. Hasty, Inter-species population dynamics enhance microbial horizontal gene transfer and spread of antibiotic resistance. *eLife* **6**, e25950 (2017). [doi:10.7554/eLife.25950](https://doi.org/10.7554/eLife.25950) [Medline](#)
20. B. Vogelstein, E. R. Fearon, S. R. Hamilton, S. E. Kern, A. C. Preisinger, M. Leppert, Y. Nakamura, R. White, A. M. Smits, J. L. Bos, Genetic alterations during colorectal-tumor development. *N. Engl. J. Med.* **319**, 525–532 (1988). [doi:10.1056/NEJM198809013190901](https://doi.org/10.1056/NEJM198809013190901) [Medline](#)
21. See supplementary materials.
22. D. J. Simpson, L. F. Dawson, J. C. Fry, H. J. Rogers, M. J. Day, Influence of flanking homology and insert size on the transformation frequency of *Acinetobacter baylyi* BD413. *Environ. Biosafety Res.* **6**, 55–69 (2007). [doi:10.1051/ebr:2007027](https://doi.org/10.1051/ebr:2007027) [Medline](#)
23. F. André, M. Arnedos, A. S. Baras, J. Baselga, P. L. Bedard, M. F. Berger, M. Bierkens, F. Calvo, E. Cerami, D. Chakravarty, K. K. Dang, N. E. Davidson, C. Del Vecchio Fitz, S. Dogan, R. N. DuBois, M. D. Ducar, P. A. Futreal, J. Gao, F. Garcia, S. Gardos, C. D. Gocke, B. E. Gross, J. Guinney, Z. J. Heins, S. Hintzen, H. Horlings, J. Hudeček, D. M. Hyman, S. Kamel-Reid, C. Kandath, W. Kinyua, P. Kumari, R. Kundra, M. Ladanyi, C. Lefebvre, M. L. LeNoue-Newton, E. M. Lepisto, M. A. Levy, N. I. Lindeman, J. Lindsay, D. Liu, Z. Lu, L. E. MacConaill, I. Maurer, D. S. Maxwell, G. A. Meijer, F. Meric-Bernstam, C. M. Micheel, C. Miller, G. Mills, N. D. Moore, P. M. Nederlof, L. Omberg, J. A. Orechia, B. H. Park, T. J. Pugh, B. Reardon, B. J. Rollins, M. J. Routbort, C. L. Sawyers, D. Schrag, N. Schultz, K. R. M. Shaw, P. Shivdasani, L. L. Siu, D. B. Solit, G. S. Sonke, J. C. Soria, P. Sripakdeevong, N. H.

- Stickle, T. P. Stricker, S. M. Sweeney, B. S. Taylor, J. J. ten Hoeve, S. B. Thomas, E. M. Van Allen, L. J. Van 'T Veer, T. van de Velde, H. van Tinteren, V. E. Velculescu, C. Virtanen, E. E. Voest, L. L. Wang, C. Wathoo, S. Watt, C. Yu, T. V. Yu, E. Yu, A. Zehir, H. Zhang; AACR Project GENIE Consortium, AACR Project GENIE: Powering Precision Medicine through an International Consortium. *Cancer Discov.* **7**, 818–831 (2017). [doi:10.1158/2159-8290.CD-17-0151](https://doi.org/10.1158/2159-8290.CD-17-0151) [Medline](#)
24. W. Li, Y. Liu, S. Cai, C. Yang, Z. Lin, L. Zhou, L. Liu, X. Cheng, W. Zeng, Not all mutations of *KRAS* predict poor prognosis in patients with colorectal cancer. *Int. J. Clin. Exp. Pathol.* **12**, 957–967 (2019). [Medline](#)
25. P. Priestley, J. Baber, M. P. Lolkema, N. Steeghs, E. de Bruijn, C. Shale, K. Duyvesteyn, S. Haidari, A. van Hoeck, W. Onstenk, P. Roepman, M. Voda, H. J. Bloemendal, V. C. G. Tjan-Heijnen, C. M. L. van Herpen, M. Labots, P. O. Witteveen, E. F. Smit, S. Sleijfer, E. E. Voest, E. Cuppen, Pan-cancer whole-genome analyses of metastatic solid tumours. *Nature* **575**, 210–216 (2019). [doi:10.1038/s41586-019-1689-y](https://doi.org/10.1038/s41586-019-1689-y) [Medline](#)
26. R. M. Cooper, J. Hasty, One-Day Construction of Multiplex Arrays to Harness Natural CRISPR-Cas Systems. *ACS Synth. Biol.* **9**, 1129–1137 (2020). [doi:10.1021/acssynbio.9b00489](https://doi.org/10.1021/acssynbio.9b00489) [Medline](#)
27. T. R. M. Lannagan, Y. K. Lee, T. Wang, J. Roper, M. L. Bettington, L. Fennell, L. Vrbanac, L. Jonavicius, R. Somashekar, K. Gieniec, M. Yang, J. Q. Ng, N. Suzuki, M. Ichinose, J. A. Wright, H. Kobayashi, T. L. Putoczki, Y. Hayakawa, S. J. Leedham, H. E. Abud, Ö. H. Yilmaz, J. Marker, S. Klebe, P. Wirapati, S. Mukherjee, S. Tejpar, B. A. Leggett, V. L. J. Whitehall, D. L. Worthley, S. L. Woods, Genetic editing of colonic organoids provides a molecularly distinct and orthotopic preclinical model of serrated carcinogenesis. *Gut* **68**, 684–692 (2019). [doi:10.1136/gutjnl-2017-315920](https://doi.org/10.1136/gutjnl-2017-315920) [Medline](#)
28. R. Lutz, H. Bujard, Independent and tight regulation of transcriptional units in *Escherichia coli* via the LacR/O, the TetR/O and AraC/I1-I2 regulatory elements. *Nucleic Acids Res.* **25**, 1203–1210 (1997). [doi:10.1093/nar/25.6.1203](https://doi.org/10.1093/nar/25.6.1203) [Medline](#)
29. C. Myhrvold, C. A. Freije, J. S. Gootenberg, O. O. Abudayyeh, H. C. Metsky, A. F. Durbin, M. J. Kellner, A. L. Tan, L. M. Paul, L. A. Parham, K. F. Garcia, K. G. Barnes, B. Chak, A. Mondini, M. L. Nogueira, S. Isern, S. F. Michael, I. Lorenzana, N. L. Yozwiak, B. L. MacInnis, I. Bosch, L. Gehrke, F. Zhang, P. C. Sabeti, Field-deployable viral diagnostics using CRISPR-Cas13. *Science* **360**, 444–448 (2018). [doi:10.1126/science.aas8836](https://doi.org/10.1126/science.aas8836) [Medline](#)
30. J. S. Chen, E. Ma, L. B. Harrington, M. Da Costa, X. Tian, J. M. Palefsky, J. A. Doudna, CRISPR-Cas12a target binding unleashes indiscriminate single-stranded DNase activity. *Science* **360**, 436–439 (2018). [doi:10.1126/science.aar6245](https://doi.org/10.1126/science.aar6245) [Medline](#)
31. Y. Zhong, F. Xu, J. Wu, J. Schubert, M. M. Li, Application of Next Generation Sequencing in Laboratory Medicine, Application of Next Generation Sequencing in Laboratory Medicine. *Ann. Lab. Med.* **41**, 25–43 (2021). [doi:10.3343/alm.2021.41.1.25](https://doi.org/10.3343/alm.2021.41.1.25) [Medline](#)
32. M. Iwamoto, J. Y. Huang, A. B. Cronquist, C. Medus, S. Hurd, S. Zansky, J. Dunn, A. M. Woron, N. Oosmanally, P. M. Griffin, J. Besser, O. L. Henao; Centers for Disease Control and Prevention (CDC), Bacterial enteric infections detected by culture-independent diagnostic tests—FoodNet, United States, 2012–2014. *MMWR Morb. Mortal. Wkly. Rep.* **64**, 252–257 (2015). [Medline](#)

33. O. Shimada, H. Ishikawa, H. Tosaka-Shimada, T. Yasuda, K. Kishi, S. Suzuki, Detection of deoxyribonuclease I along the secretory pathway in Paneth cells of human small intestine. *J. Histochem. Cytochem.* **46**, 833–840 (1998). [doi:10.1177/002215549804600706](https://doi.org/10.1177/002215549804600706) [Medline](#)
34. A. Wilcks, A. H. A. M. van Hoek, R. G. Joosten, B. B. L. Jacobsen, H. J. M. Aarts, Persistence of DNA studied in different ex vivo and in vivo rat models simulating the human gut situation. *Food Chem. Toxicol.* **42**, 493–502 (2004). [doi:10.1016/j.fct.2003.10.013](https://doi.org/10.1016/j.fct.2003.10.013) [Medline](#)
35. T. Netherwood, S. M. Martín-Orúe, A. G. O’Donnell, S. Gockling, J. Graham, J. C. Mathers, H. J. Gilbert, Assessing the survival of transgenic plant DNA in the human gastrointestinal tract. *Nat. Biotechnol.* **22**, 204–209 (2004). [doi:10.1038/nbt934](https://doi.org/10.1038/nbt934) [Medline](#)
36. M. O. Din, T. Danino, A. Prindle, M. Skalak, J. Selimkhanov, K. Allen, E. Julio, E. Atolia, L. S. Tsimring, S. N. Bhatia, J. Hasty, Synchronized cycles of bacterial lysis for in vivo delivery. *Nature* **536**, 81–85 (2016). [doi:10.1038/nature18930](https://doi.org/10.1038/nature18930) [Medline](#)
37. G. D. Sepich-Poore, L. Zitvogel, R. Straussman, J. Hasty, J. A. Wargo, R. Knight, The microbiome and human cancer. *Science* **371**, eabc4552 (2021). [doi:10.1126/science.abc4552](https://doi.org/10.1126/science.abc4552) [Medline](#)
38. S. C. Pearce, R. L. McWhinnie, F. E. Nano, Synthetic temperature-inducible lethal gene circuits in Escherichia coli. *Microbiology (Reading)* **163**, 462–471 (2017). [doi:10.1099/mic.0.000446](https://doi.org/10.1099/mic.0.000446) [Medline](#)
39. T. Sato, D. E. Stange, M. Ferrante, R. G. J. Vries, J. H. Van Es, S. Van den Brink, W. J. Van Houdt, A. Pronk, J. Van Gorp, P. D. Siersema, H. Clevers, Long-term expansion of epithelial organoids from human colon, adenoma, adenocarcinoma, and Barrett’s epithelium. *Gastroenterology* **141**, 1762–1772 (2011). [doi:10.1053/j.gastro.2011.07.050](https://doi.org/10.1053/j.gastro.2011.07.050) [Medline](#)
40. C. Becker, M. C. Fantini, M. F. Neurath, High resolution colonoscopy in live mice. *Nat. Protoc.* **1**, 2900–2904 (2006). [doi:10.1038/nprot.2006.446](https://doi.org/10.1038/nprot.2006.446) [Medline](#)
41. K. P. O’Rourke, E. Loizou, G. Livshits, E. M. Schatoff, T. Baslan, E. Manchado, J. Simon, P. B. Romesser, B. Leach, T. Han, C. Pauli, H. Beltran, M. A. Rubin, L. E. Dow, S. W. Lowe, Transplantation of engineered organoids enables rapid generation of metastatic mouse models of colorectal cancer. *Nat. Biotechnol.* **35**, 577–582 (2017). [doi:10.1038/nbt.3837](https://doi.org/10.1038/nbt.3837) [Medline](#)